AGU PUBLICATIONS

Space Weather

RESEARCH ARTICLE
10.1002/2015SW001208

Key Points:
- We model dose rates and accumulated doses for the 23 July 2012 SEP event
- Peak dose rate is very large, but total dose is comparable to previous events
- We show how the position of the observer relative to ICME affects observed dose

Correspondence to:
C. J. Joyce,
cjl46@unh.edu

Citation:
Joyce, C. J., et al. (2015), Analysis of the potential radiation hazard of the 23 July 2012 SEP event observed by STEREO A using the EMMREM model and LRO/CRaTER, *Space Weather*, *13*, 560–567, doi:10.1002/2015SW001208.

Received 22 APR 2015
Accepted 10 AUG 2015
Accepted article online 14 AUG 2015
Published online 11 SEP 2015

Analysis of the potential radiation hazard of the 23 July 2012 SEP event observed by STEREO A using the EMMREM model and LRO/CRaTER

C. J. Joyce[1], N. A. Schwadron[1], L. W. Townsend[2], R. A. Mewaldt[3], C. M. S. Cohen[3], T. T. von Rosenvinge[4], A. W. Case[5], H. E. Spence[1], J. K. Wilson[1], M. Gorby[1], M. Quinn[1], and C. J. Zeitlin[6]

[1]Physics Department, Space Science Center, University of New Hampshire, Durham, New Hampshire, USA, [2]Department of Nuclear Engineering, The University of Tennessee, Knoxville, Knoxville, Tennessee, USA, [3]California Institute of Technology, Pasadena, California, USA, [4]Laboratory for High Energy Astrophysics, NASA/Goddard Space Flight Center, Greenbelt, Maryland, USA, [5]Harvard-Smithsonian Center for Astrophysics, Cambridge, Massachusetts, USA, [6]Southwest Research Institute, Boulder, Colorado, USA

Abstract We present a study of the potential radiation hazard of the powerful, superfast interplanetary coronal mass ejection (ICME) observed by STEREO A on 23 July 2012. Using energetic proton flux data from the High Energy Telescope and Low Energy Telescope instruments aboard STEREO A together with the Earth-Moon-Mars Radiation Environment Module, we compute dose rates and accumulated doses during the event for both skin/eye and blood forming organs using four physically relevant levels of shielding. For spacesuit equivalent shielding, we compute a peak skin/eye dose rate of 1970 cGy-Eq/d, a value far greater than those of the 2003 Halloween storms or the January and March solar energetic particle events of 2012. However, due to the relative brevity of the event, the resulting accumulated dose was just 383 cGy-Eq, which is more aligned with the total doses of the 2003 Halloween and 2012 January/March events. Additionally, we use dose rates at STEREO B and Lunar Reconnaissance Orbiter/Cosmic Ray Telescope for the Effects of Radiation (LRO/CRaTER) during the event to show how the radiation impact is affected by the position of the ICME relative to the observer. Specifically, we find that the energetic particle event associated with the local shock and ICME passage at STEREO A caused greatly enhanced dose rates when compared to STEREO B and LRO/CRaTER, which were longitudinally distant from the ICME. The STEREO A/B dose rates used here will soon be made available to the community as a tool for studying the energetic particle radiation of solar events from different longitudes as a part of NASA's Heliophysics Virtual Observatories and on the Predictions of radiation from REleASE, EMMREM, and Data Incorporating CRaTER, COSTEP, and other SEP measurements (PREDICCS) and CRaTER websites.

1. Introduction

On 23 July 2012, an unusually fast and powerful interplanetary coronal mass ejection (ICME) was observed in situ by the Solar Terrestrial Relations Observatory Ahead (STEREO A) spacecraft [*Kaiser et al.*, 2008]. Besides its record speed (2780 km/s) and exceptionally strong magnetic field (109 nT at maximum) [*Russell et al.*, 2013], this event was also unique in that it did not show evidence of a fast-mode shock at its bow, a feature commonly associated with large ICMEs [*Gopalswamy*, 2007]. *Russell et al.* [2013] provided an analysis of the magnetic field, plasma, and energetic particle conditions during the event, finding that the extremely high pressures exerted by the energetic particles within the ICME served to alter the plasma conditions in such a way as to produce a subsonic interaction with slow-mode leading bow waves. *Russell et al.* [2013] proposed that while this effect could limit the potential harm caused by such an event encountering the Earth, the strength and southward orientation of the magnetic field combined with the high speed of the ICME would likely result in a powerful geomagnetic storm. This event has been the subject of several subsequent studies, including those that model the propagation and arrival time of the ICME [*Liou et al.*, 2014; *Temmer and Nitta*, 2015] and those attempting to determine the potential magnetospheric impact of the event had it been Earth-bound [*Baker et al.*, 2013; *Ngwira et al.*, 2013].

Solar energetic particles (SEPs) accelerated at the shock fronts of ICMEs represent a major radiation threat to astronauts in interplanetary space. The 23 July 2012 event provides a unique opportunity to study the

radiation impact of an exceptionally powerful ICME. In this study, we provide an analysis of the potential harm this event may have caused had it encountered astronauts during its transit through the heliosphere. We utilize flux measurements of energetic protons ranging from 1.8–100 MeV recorded by the Low Energy Telescope (LET) [*Mewaldt et al.*, 2008] and High Energy Telescope (HET) [*Rosenvinge et al.*, 2008] instruments aboard STEREO A during the event together with the Earth-Moon-Mars Radiation Environment Module (EMMREM) [*Schwadron et al.*, 2010] to produce time series of dose rates and accumulated doses for skin/eye (equivalent to 1 g/cm^2 H_2O) as well as blood-forming organs (BFO, which primarily represents bone marrow and is equivalent to 10 g/cm^2 H_2O). These dose rates and accumulated doses are multiplied by the Relative Biological Effectiveness (1.5 for protons), which scales different forms of radiation based on their biological damage potential [*Townsend et al.*, 2013]. Due to the difficulty in extrapolating the energetic particle intensities measured by the HET instrument to a full field of view without detailed information about the particle anisotropy, we simply assume that the radiation is isotropic. Therefore, the computed dose rates shown here represent an upper limit which may be greater than the actual dose rate depending on the degree of anisotropy along the nominal Parker spiral that the HET measures from. This is also true for previous events that have been modeled using EMMREM with GOES data as input. The dose rates shown here are computed for different levels of shielding and are compared to NASA Permissible Exposure Limits in order to gauge the potential threat this event might have posed to astronauts [*NASA Space Flight*, 2007]. We also provide a comparison to three recent large SEP events in order to give a sense of the relative severity of the event. For our purposes, we consider periods containing multiple peaks associated with different ICMEs and/or flares in close temporal proximity to one another, for example, the five peaks of the 2003 Halloween Storms, to be part of a single space weather event.

Finally, we provide an analysis of the longitudinal variation of the radiation impact of this event using additional dose rate data computed at STEREO B and the Cosmic Ray Telescope for the Effects of Radiation (CRaTER) [*Spence et al.*, 2010] aboard the Lunar Reconnaissance Orbiter (LRO) [*Chin et al.*, 2007]. During this event, STEREO A/B and LRO were ideally positioned to show how the location of an observer relative to the ICME affects the radiation conditions observed during a powerful solar event. Using simulations of the event performed by the Community Coordinated Modeling Center (CCMC) with the validated Wang-Sheeley-Arge-ENLIL+Cone model [*Spence et al.*, 2004; *Owens et al.*, 2005, 2008; *Case et al.*, 2008], we are able to show how the measured dose rates at the three observers change as the ICME propagates outward from the Sun.

2. Computed Dose Rates at STEREO A During the 23 July 2012 Event and Comparison to Previous Events

EMMREM is a numeric model designed to characterize the radiation environment of the inner heliosphere by solving for the temporal and spatial evolution of energetic particle distributions and computing energetic particle fluxes and dose rates at different locations of interest including the Earth, Moon, and Mars, as well as interplanetary space [*Schwadron et al.*, 2010]. Validation of the EMMREM radiation model as a component of the online PREDICCS system is provided by *Joyce et al.* [2013], who used measurements from LRO/CRaTER during three major solar events in 2012 to show that EMMREM provides accurate modeling of radiation from SEP events near the Moon and in interplanetary space, computing dose rates with an average error of 17.6% and accumulated doses with an average error of 24.9%.

For this analysis, we use the Baryon Transport Module (BRYNTRN) [*Wilson et al.*, 1991], a submodule of EMMREM, to compute dose rates at STEREO A by solving for the transport of protons and secondary particles through various shielding materials and thicknesses, using flux data from the LET/HET as input. The flux data used here have been modified for use in a future publication [Mewaldt et al., in preparation] in order to correct for certain instrumental effects that resulted in inaccurate measurements in some of the lower energy bins of the HET during the peak hour of the event and have been used in this study to improve the accuracy of our analysis. EMMREM takes flux measurements made by the LET/HET instruments at discrete energies from 1.8–100 MeV and converts them into a continuous spectrum using logarithmic interpolation, with the interpolation between the two highest-energy data points being used to extend the spectrum to GeV levels. Given its success in modeling previous events, we expect BRYNTRN to model the potential radiation threat of the July 2012 event to astronauts in interplanetary space with reasonable accuracy.

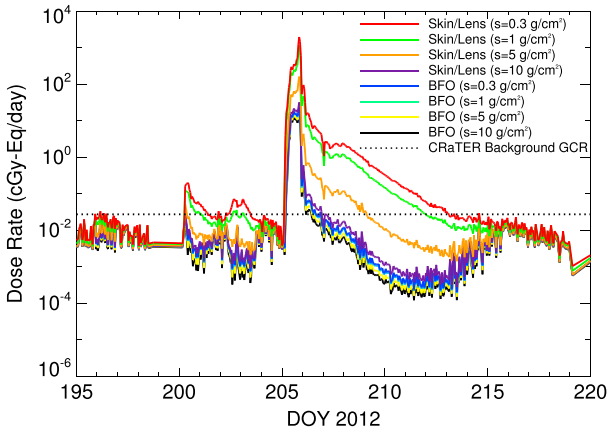

Figure 1. Dose rates during the July 2012 SEP event as computed by the EMMREM radiation module using HET/LET data from STEREO A. Dose rates are computed for skin/eye as well as BFO for four levels of shielding, s, corresponding to spacesuit, heavy spacesuit, spacecraft, and heavy protective shielding. The peak dose rate occurs on 23 July at 20:00UT. A dotted line plots the average background GCR dose rate before and after the event as measured by the CRaTER instrument aboard LRO.

Figure 1 shows dose rates computed with BRYNTRN using STEREO A data during the July 2012 event for both skin/eye and BFO. Dose rates are computed through aluminum shielding of 0.3, 1.0, 5.0, and 10.0 g/cm^2, corresponding to spacesuit, heavy spacesuit, spacecraft, and heavy protective shielding, respectively. Because BRYNTRN computes dose rates using only protons and their secondaries; it is not accurate in predicting the dose rate during quiet times when heavier galactic cosmic rays (GCRs) contribute significantly to the absorbed radiation. For this reason, Figure 1 also shows the average background GCR rate measured by the CRaTER spacecraft during quiet times before and after the event. This background GCR rate is the D1D2 dose rate described by *Schwadron et al.* [2012], which is comparable to the computed skin/eye dose shown here for the lowest level of shielding and provides a better sense of when the radiation environment is dominated by SEPs.

Figure 2 shows the accumulated dose rates for skin/eye and BFO for each level of shielding during the event. We see that for the lowest two levels of shielding, the accumulated dose exceeds both the skin and lens 30 day dose limits for astronauts set by NASA [*Townsend et al.*, 2013]. The 30 day BFO dose limit is not exceeded for even the lowest level of shielding. We compute all dose rates and accumulated doses for 2π steradian exposure where half the sky is blocked, as it would be on or near the surface of a planet, so that our results are directly comparable to data from previous events.

Table 1 shows the peak dose rates and accumulated doses for skin/eye and BFO with the four different levels of shielding. The hourly dose rate for spacesuit shielding peaks at approximately 1970 cGy-Eq/d, almost four times as large as the peak rate computed by EMMREM for the 2003 Halloween Storms (~500 cGy-Eq/d) [*Schwadron et al.*, 2010] and more than an order of magnitude greater than the peak dose rates computed by EMMREM for the January (140 cGy-Eq/d) and March (167 cGy-Eq/d) events of 2012 [*Joyce et al.*, 2013]. While the peak dose rate for this event is much higher than the previous events, it lasted for only an hour, whereas the previous events maintained dose rates at or near the peak levels for a day or more and also contained multiple peaks. As a result, the dose accumulated at the spacesuit level of shielding for the event is just 383 cGy-Eq, which is somewhat smaller than the 2003 Halloween event (~400 cGy-Eq) but still significantly greater than the 2012 events (177 cGy-Eq for January and 228 cGy-Eq for March). Errors are computed by using the uncertainties in the flux spectra to create upper and lower bound spectra and inserting them into the model.

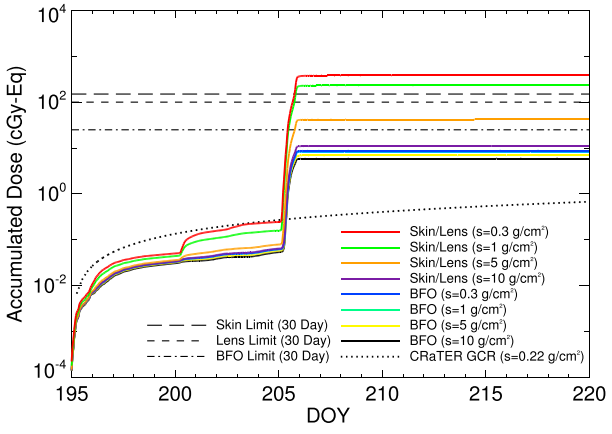

Figure 2. Accumulated doses for the July 2012 SEP event as computed by the EMMREM radiation module. Doses are computed for skin/eye as well as BFO for various levels of shielding. Also indicated on the plot are the 30 day NASA dose limits for skin, eye, and BFO, as well as the dose accumulated for the CRaTER GCR rate shown in Figure 1.

Table 1. Peak Dose Rates and Accumulated Doses for Skin/Eye and BFO for the July 2012 STEREO Event as Computed by the EMMREM Radiation Module[a]

	Skin/Eye		
Shielding (g/cm^2)	Peak Dose Rate (cGy-Eq/d)	Accumulated Dose (cGy-Eq)	Band Fct. Dose (cGy-Eq)
0.3	1970 ± 35.0	383 ± 4.73	401 ± 36.7
1.0	1140 ± 19.1	233 ± 2.63	241 ± 24.0
5.0	162 ± 3.87	41.8 ± 0.55	38.4 ± 5.00
10.0	31.9 ± 1.05	11.0 ± 0.16	9.38 ± 1.36
		BFO	
0.3	23.4 ± 0.81	8.69 ± 0.13	6.26 ± 0.92
1.0	21.8 ± 0.77	8.25 ± 0.13	5.48 ± 0.80
5.0	17.3 ± 0.64	6.88 ± 0.10	2.86 ± 0.42
10.0	14.1 ± 0.53	5.84 ± 0.09	1.51 ± 0.22

[a]Accumulated doses computed using a Band function fit to the HET/LET flux data as input into BRYNTRN rather than the log interpolation used for the other data are also shown. Doses are computed for four different levels of shielding corresponding to spacesuit, heavy spacesuit, spacecraft, and heavy protective shielding.

Also shown in the table are accumulated doses computed using a Band function [*Band et al.*, 1993] fit to the HET/LET fluence spectrum of the event as input into the BRYNTRN model, as opposed to the log interpolation data. The Band function fit as well as the measured fluence spectrum and the log interpolated fluence spectrum are shown in Figure 3. We see that using the Band function fit results in very similar skin/eye doses, being somewhat larger at the two lower levels of shielding and slightly smaller at the two heavier levels of shielding. For BFO, the Band function fit results in somewhat lower dose rates overall. This is due to the Band function fit having a greater proportion of lower energy protons, which contribute the majority of the dose for low levels of shielding, whereas the log interpolated spectrum has greater fluences at higher energies, which penetrate shielding more effectively allowing them to contribute more radiation to BFO and for higher levels of shielding.

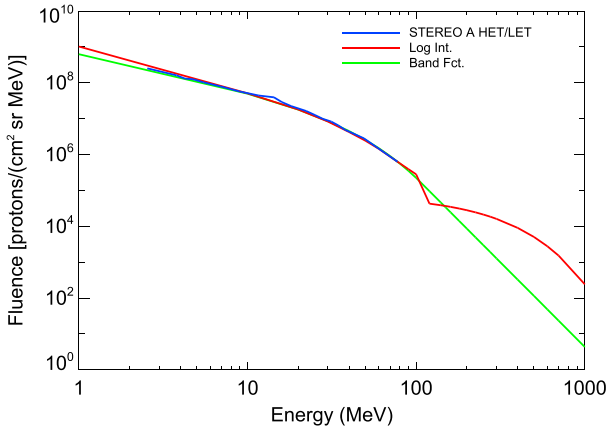

Figure 3. Fluence spectra during the 23 July 2012 solar event for STEREO HET/LET as well as the log interpolation and Band function fits used here to compute dose rates and accumulated doses. The Band function fit is applied to the measured fluence spectrum for the event, while the log interpolation is applied to the measured flux spectra at each time step and then summed to get the plotted fluence spectrum, resulting in the irregular features seen at higher energies.

3. Longitudinal Variation of Radiation Impact

During this event, the STEREO A, STEREO B, and LRO spacecraft were ideally positioned to show how observed radiation levels are affected by the location of the observer relative to the ICME. Figure 4 shows the output of the WSA-ENLIL+Cone model, computed by the CCMC for this event. The plot shows the radially scaled density profile of the inner heliosphere as well as the interplanetary magnetic field lines connecting the Sun to various points of interest at 1 AU, including STEREO A, STEREO B, and Earth (LRO/CRaTER), at four different times during the event. From this plot, we get a clear sense of how the ICME evolves outward from the Sun and how well each observer is magnetically connected to the shock front at each stage.

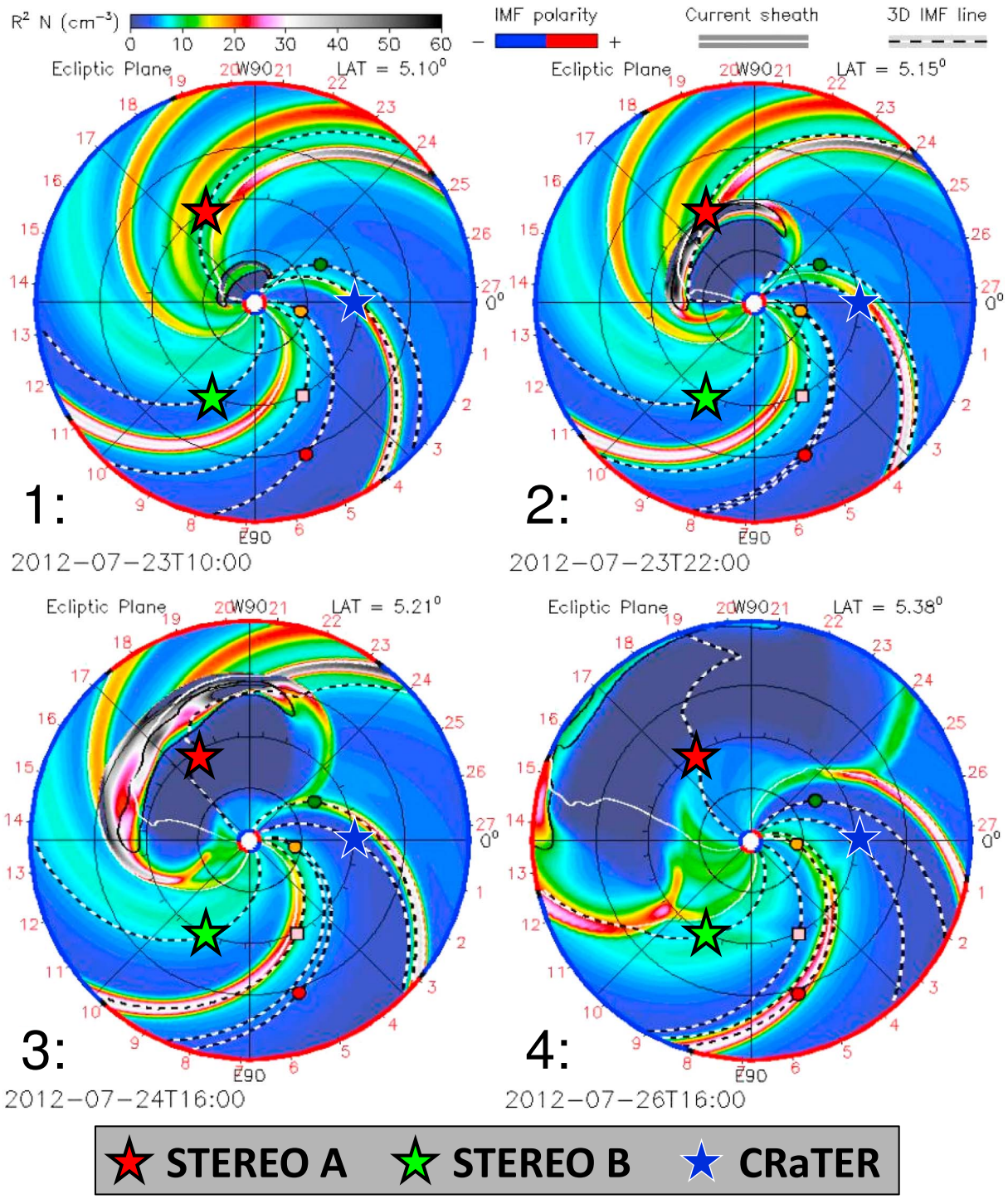

Figure 4. Output of the WSA-ENLIL+Cone model as computed by the CCMC during the 23 July 2012 solar event. Radially scaled density profiles are shown at four different times during the event. Also shown are interplanetary magnetic field lines connecting to various points of interest including STEREO A, STEREO B, and Earth/LRO/CRaTER. The positions of STEREO A/B and CRaTER as well as their magnetic connection to the ICME during the event can be used to better understand the radiation observed by each spacecraft. Data from this run were originally presented by *Zheng et al.* [2014].

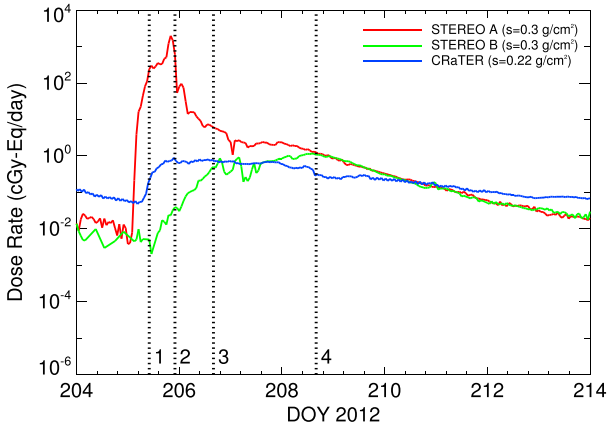

Figure 5. Dose rates at STEREO A/B and LRO/CRaTER during the 23 July 2012 solar event. Plot includes time labels corresponding to the four plots in Figure 4. At time 1, STEREO A and CRaTER see sharp increases in dose rate due to their magnetic connection to the CME while it is still relatively close to the Sun. At time 2, the dose rate at STEREO A has peaked due to the arrival of the shock. At time 3, the STEREO A dose rate has dropped off significantly following the passage of the shock, while the radiation at STEREO B gradually increases. At time 4, the STEREO B dose rate has peaked due to magnetic connection to the ICME from behind.

Figure 5 shows the dose rates during the event at STEREO A/B and LRO, where the STEREO B dose rate is computed in the same manner as with STEREO A and the LRO dose rate is the previously described CRaTER D1D2 rate. The four simulation time periods shown in Figure 4 are labeled on the dose rate plot to show how the evolving conditions impact the dose rates at each spacecraft. Table 2 shows the peak times, peak dose rates, and total accumulated doses for the three spacecraft. We see that the amount of time that passes before the peak is reached varies by almost 3 days, while the accumulated doses and peak dose rates vary by more than 2 and 3 orders of magnitude, respectively.

The observed behavior of the dose rates is consistent with the findings of *Reames* [1999], who showed how proton intensities varied depending on the position of the observer relative to the ICME. Assuming that particle acceleration is greatest at the nose of the ICME and declines toward its flanks, *Reames* [1999] identified three common characterizations of energetic particle observations based on the observed intensity-time profiles. Figure 6 combines the graphics of Figure 4 with the dose rate time series of Figure 5 in order to provide a clearer illustration of this effect.

The first type of intensity profile is observed by spacecraft on the eastern flank of the shock, in this case LRO/CRaTER. The observer is magnetically connected to the nose of the shock early in the event when the CME is still close to the Sun; however, the connection moves toward the flank as the ICME propagates outward, resulting in a steep initial jump in particle intensities that decreases gradually as the event progresses in time. This is very similar to the behavior observed by CRaTER during this event, except that CRaTER is initially connected closer to the flank of the ICME, resulting in a more modest initial jump. Interestingly, the Earth passed through an apparent corotating interaction region during the time of the elevated dose rates which likely worked to beam energetic particles from the ICME to CRaTER.

The second type of observation occurs for centrally located spacecraft (in this case STEREO A), which tend to not be well connected to the nose early in the event, resulting in a more gradual rise in particle intensities as the ICME approaches, followed by a sharp dropoff once it has passed. Due to the wide longitudinal extent of the July 2012 CME, STEREO A was well connected to the shock front during even the early stages of the event, resulting in an intense initial increase in the dose rate. The dose rate did not reach its absolute peak, however, until the spacecraft encountered the shock, which was then followed by the characteristic dropoff once it had passed.

The final type of observation is made by spacecraft on the western flank of the shock (STEREO B), which are not initially well connected to the shock front and thus see the most gradual increase in particle intensities,

Table 2. Peak Dose Times, Peak Dose Rates, and Total Accumulated Doses for CRaTER and STEREO A/B During the 23 July 2012 Event, Indicating How the Longitudinal Position of the Spacecraft Relative to the ICME Affects the Observed Radiation

	CRaTER	STEREO A	STEREO B
Peak Hour (UT)	23 July 21:00	23 July 20:00	26 July 14:00
Peak Dose Rate (cGy-Eq/d)	0.89	1970	1.17
Accumulated Dose (cGy-Eq)	2.94	383	2.83

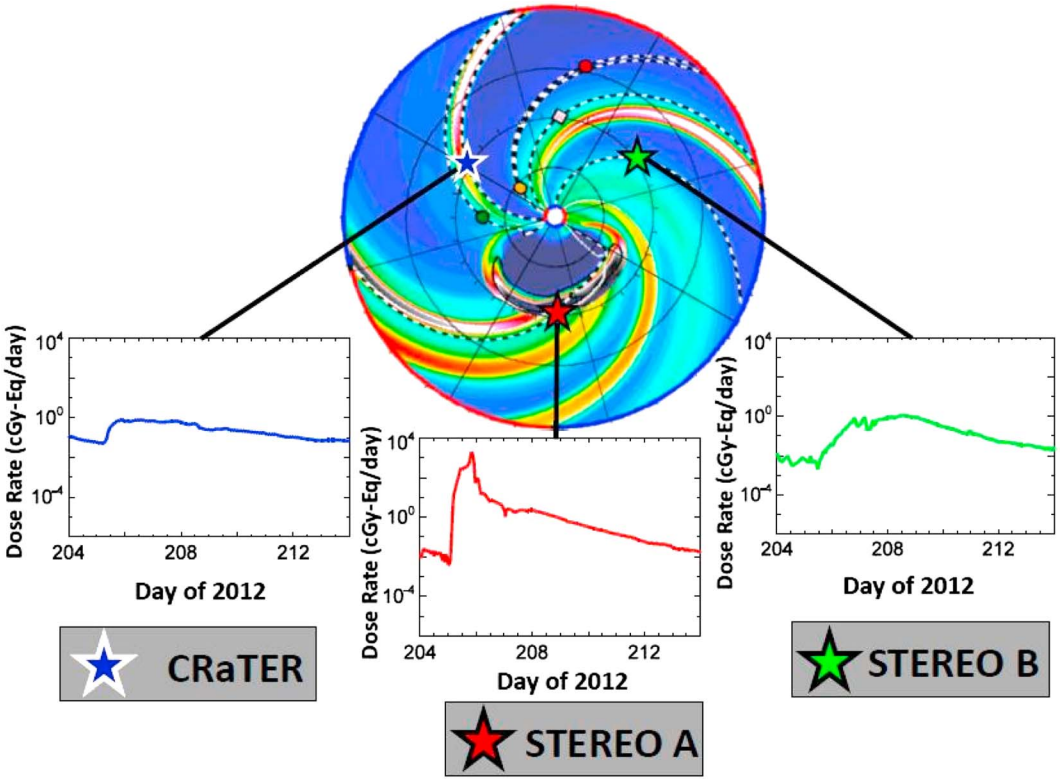

Figure 6. Illustration of the characterizations observed by *Reames* [1999], using the ENLIL model output at the time the shock arrives at 1AU and the dose rates observed at CRaTER, STEREO A, and STEREO B, representing the observers located at the eastern flank, center, and western flank of the shock front, respectively. A short video showing the evolution of the CME and dose rates during the event with an accompanying sonification of the data is available on the Sun 2 Ice multimedia page at: http://sun-2-ice.sr.unh.edu/multimedia.html.

reaching their peak well after the shock has passed (i.e., radially beyond 1 AU), when the observer is magnetically connected to the nose from behind. STEREO B data for this event conform to expectations in this case, having the slowest increase in dose rate of any of the three spacecraft, not reaching the levels seen by CRaTER until almost 2 days into the event and not peaking until more than 3 days in, after which STEREO A and B had almost identical dose rates. This is likely due to the reservoir effect, which is characterized by virtually identical flux spectra observed over wide longitudinal intervals following the passage of shocks associated with large ICMEs [*Reames et al.*, 1997, 1996].

4. Conclusion

The 23 July 2012 STEREO A event offers a unique opportunity to assess the potential radiation threat of an exceptionally powerful CME. We find that the peak dose rate greatly exceeds those of the 2003 Halloween Storms and the January/March events of 2012, while the relative brevity of the event results in a total accumulated dose that is comparable to the largest of those events. While the total dose is not as high as might initially be expected for such an intense event, the amount of radiation that would be absorbed by the crew of a spacecraft during such an event is substantial, even with the benefit of heavy protective shielding throughout, and would be significantly worse in interplanetary space where the full field of view would double the absorbed doses shown in Table 1. This is especially true when viewed in the context of a longer mission where incessant GCRs and additional episodic SEP events would only make the cumulative radiation effects worse.

Our analysis of dose rates at three different longitudes at 1 AU during the event demonstrates how dramatically the radiation impact is affected by the position of the spacecraft relative to the evolving ICME. Depending on the location of the observer, we see that the peak dose rate varies by more than 3 orders of magnitude and the amount of time before the peak is reached can be anywhere between 1 and 3 days. Upon initial analysis, the observed dose rates are in good agreement with expectations based on previous observations made

by *Reames* [1999]; however, additional modeling may be required to fully quantify these effects. The capability of measuring dose rates at three different longitudes represents a new way to study solar events and time series of the STEREO A/B and CRaTER dose rates shown here are in the process of being incorporated into a data set that will be made available to the community as a part of NASA's Heliophysics Virtual Observatories, as well as on the PREDICCS and CRaTER websites (http://prediccs.sr.unh.edu/ and http://crater-web.sr.unh.edu/).

Acknowledgments
This work is supported by NASA LRO/CRaTER/PREDICCS Project (contract NNG11PA03C), the NSF/FESD Sun-to-Ice Project (grant AGS1135432), and the NASA/LWS/NSF EMMREM Project (grant NNX11AC06G). The work on the corrected STEREO A HET spectrum was performed at Caltech and was supported by NASA grants NNX11A075G and subcontract SA2715-26309 from UC Berkeley under NASA Contract NAS5-003131. We thank the STEREO HET and LET instrument teams for providing the STEREO data used here (available at: http://www.srl.caltech.edu/STEREO/index.html). Simulation results have been provided by the Community Coordinated Modeling Center at Goddard Space Flight Center through their public Runs on Request system (http://ccmc.gsfc.nasa.gov). The CCMC is a multiagency partnership between NASA, AFMC, AFOSR, AFRL, AFWA, NOAA, NSF, and ONR. The ENLIL+Cone Model was developed by Dusan Odstrcil at the University of Colorado at Boulder. The CRaTER data used here are available on the CRaTER website: http://crater-web.sr.unh.edu/.

References

Baker, D. N., X. Li, A. Pulkkinen, C. M. Ngwira, M. L. Mays, A. B. Galvin, and K. D. C. Simunac (2013), A major solar eruptive event in July 2012: Defining extreme space weather scenarios, *Space Weather*, *11*, 585–591, doi:10.1002/swe.20097.

Band, D., et al. (1993), BATSE observations of gamma-ray burst spectra. I—Spectral diversity, *Astrophys. J.*, *413*, 281–292.

Case, A. W., H. E. Spence, M. J. Owens, P. Riley, and D. Odstrcil (2008), Ambient solar wind's effect on ICME transit times, *Geophys. Res. Lett.*, *35*, L15105, doi:10.1029/2008GL034493.

Chin, G., et al. (2007), Lunar reconnaissance orbiter overview: The instrument suite and mission, *Space Sci. Rev.*, *129*(4), 391–419.

Gopalswamy, N. (2007), Properties of interplanetary coronal mass ejections, in *Solar Dynamics and Its Effects on the Heliosphere and Earth, Space Sci. Ser. of ISSI*, vol. 22, pp. 145–168, Springer, New York., doi:10.1007/978-0-387-69532-7_11.

Joyce, C. J., et al. (2013), Validation of PREDICCS using LRO/CRaTER observations during three major solar events in 2012, *Space Weather*, *11*, 350–360, doi:10.1002/swe.20059.

Kaiser, M. L., T. A. Kucera, J. M. Davila, O. C. St. Cyr, M. Guhathakurta, and E. Christian (2008), The STEREO mission: An introduction, *Space Sci. Rev.*, *136*(1–4), 5–16.

Liou, K., C.-C. Wu, M. Dryer, S.-T. Wu, N. Rich, S. Plunkett, L. Simpson, C. D. Fry, and K. Schenk (2014), Global simulation of extremely fast coronal mass ejection on 23 July 2012, *J. Atmos. Sol. Terr. Phys.*, *121*, 32–41, doi:10.1016/j.jastp.2014.09.013.

Mewaldt, R. A., et al. (2008), The Low-Energy Telescope (LET)and SEP central electronics for the STEREO mission, *Space Sci. Rev.*, *136*, 285–362, doi:10.1007/s11214-007-9288-x.

NASA Space Flight (2007), Human System Standard Volume 1: Crew Health, NASA-STD-3001, National Aeronautics and Space Administration, Washington, D. C.

Ngwira, C. M., A. Pulkkinen, M. Leila Mays, M. M. Kuznetsova, A. B. Galvin, K. Simunac, D. N. Baker, X. Li, Y. Zheng, and A. Glocer (2013), Simulation of the 23 July 2012 extreme space weather event: What if this extremely rare CME was Earth directed?, *Space Weather*, *11*, 671–679, doi:10.1002/2013SW000990.

Owens, M. J., C. N. Arge, H. E. Spence, and A. Pembroke (2005), An event-based approach to validating solar wind speed predictions: High speed enhancements in the Wang-Sheeley-Arge model, *J. Geophys. Res.*, *110*, A12105, doi:10.1029/2005JA01134.

Owens, M. J., H. E. Spence, S. McGregor, W. J. Hughes, J. M. Quinn, C. N. Arge, P. Riley, J. Linker, and D. Odstrcil (2008), Metrics for solar wind prediction models: Comparison of empirical, hybrid, and physics-based schemes with 8 years of L1 observations, *Space Weather*, *6*, S08001, doi:10.1029/2007SW000380.

Reames, D. V. (1999), Particle acceleration at the Sun and in the heliosphere, *Space Sci. Rev.*, *90*(3-4), 413–491.

Reames, D. V., L. M. Barbier, and C. K. Ng (1996), The spatial distribution of particles accelerated by coronal mass ejection-driven shocks, *Astrophys. J.*, *466*, 473–486.

Reames, D. V., S. W. Kahler, and C. K. Ng (1997), Spatial and temporal invariance in the spectra of energetic particles in gradual solar events, *Astrophys. J.*, *491*, 414–420.

Rosenvinge, T. T. V., et al. (2008), The high energy telescope for STEREO, *Space Sci. Rev.*, *136*(1), 391–435, doi:10.1007/s11214-007-9300-5.

Russell, C. T., et al. (2013), The very unusual interplanetary coronal mass ejection of 2012 July 23: A blast wave mediated by solar energetic particles, *Astrophys J.*, *770*, 38, doi:10.1088/0004-637X/770/1/38.

Schwadron, N. A., et al. (2010), Earth-Moon-Mars radiation environment module framework, *Space Weather*, *8*, S00E02, doi:10.1029/2009SW000523.

Schwadron, N. A., et al. (2012), Lunar radiation environment and space weathering from the Cosmic Ray Telescope for the Effects of Radiation (CRaTER), *J. Geophys. Res.*, *117*, E00H13, doi:10.1029/2011JE003978.

Spence, H. E., D. Baker, A. Burns, T. Guild, C.-L. Huang, G. Siscoe, and R. Weigel (2004), CISM metrics plan and initial model validation results, *J. Atmos. Sol. Terr. Phys.*, *66*, 1499–1507.

Spence, H. E., et al. (2010), CRaTER: The cosmic ray telescope for the effects of radiation experiment on the lunar reconnaissance orbiter mission, *Space Sci. Rev.*, *150*, 243–284, doi:10.1007/s11214-009-9584-8.

Temmer, M., and N. V. Nitta (2015), Interplanetary propagation behavior of the fast coronal mass ejection on 23 July 2012, *Sol. Phys.*, *290*(3), 919–932, doi:10.1007/s11207-014-0642-3.

Townsend, L. W., J. A. Anderson, A. M. Adamczyk, and C. M. Werneth (2013), Estimates of Carrington-class solar particle event radiation exposures as a function of altitude in the atmosphere of Mars, *Acta Astronaut.*, *89*, 189–194, doi:10.1016/j.actaastro.2013.04.010.

Wilson, J. W., L. W. Townsend, W. S. Schimmerling, G. S. Khandelwal, F. S. Khan, J. E. Nealy, F. A. Cucinotta, L. C. Simonsen, J. L. Shinn, and J. W. Norbury (1991), Transport methods and interactions for space radiations, *NASA Tech. Rep. RP-1257*, National Aeronautics and Space Administration, Office of Management, Scientific and Technical Information Program, Washington, D. C.

Zheng, Y., M. M. Kuznetsova, A. A. Pulkkinen, M. M. Maddox, and M. L. Mays (2014), Research-based monitoring, prediction, and analysis tools of the spacecraft charging environment for spacecraft users, paper presented at Spacecraft Charging Technology Conference, Pasadena, Calif., 23-27 Jun.